

## Spectral and Thermal properties of Ho<sup>3+</sup> ions doped Zinc Lithium Alumino Potassiumniobate Borophosphate Glasses

S.L. Meena

Ceramic Laboratory, Department of Physics, Jai Narain Vyas University, Jodhpur 342001(Raj.) India

\*Corresponding Author E-Mail: shankardiya7@rediffmail.com

<https://doi.org/10.30731/ijcps.10.5.2021.8-17>

### Abstract

*Glass of the system: (35-x) P<sub>2</sub>O<sub>5</sub>: 10ZnO: 10Li<sub>2</sub>O: 10Al<sub>2</sub>O<sub>3</sub>: 10K<sub>2</sub>O: 10Nb<sub>2</sub>O<sub>3</sub>: 15B<sub>2</sub>O<sub>3</sub>: xHo<sub>2</sub>O<sub>3</sub>. (Where x=1, 1.5,2 mol %) have been prepared by melt-quenching method. The amorphous nature of the prepared glass samples was confirmed by X-ray diffraction. Optical absorption, Excitation, fluorescence and Thermal spectra were recorded at room temperature for all glass samples. Judd-Ofelt intensity parameters  $\Omega_{\lambda}$  ( $\lambda=2, 4$  and  $6$ ) are evaluated from the intensities of various absorption bands of optical absorption spectra. Using these intensity parameters various radiative properties like spontaneous emission probability ( $A$ ), branching ratio ( $\beta$ ), radiative life time ( $\tau_R$ ) and stimulated emission cross-section ( $\sigma_p$ ) of various emission lines have been evaluated.*

**Keywords:** ZLAPNBP Glasses, Optical Properties, Judd-Ofelt Theory, Transmittance Properties.

### Introduction:

The rare earth ions doped glasses are used in making up conversion lasers due to their potential applications in variety of fields namely, optical data storage, display technology, undersea transmission and medical diagnostics [1-5]. Phosphate glasses are known to be low melting, optical data transmission, detection, laser, high homogeneity, good corrosion resistance, excellent chemical durability and low glass transition temperature ( $T_g$ ), better thermal stability, high thermal expansion coefficient, low phonon energy, wide optical transmission region and high refractive index materials, therefore considered to be potential nonlinear materials [6-10]. The high gain density in phosphate glasses is due to high solubility of rare earth ions in phosphate network. These glasses have high luminescence efficiency and they lack thermal lensing effects. When compared with borate and silicate glasses these glasses have distinction optical properties such as large infrared transmission window, high gain density, low up conversion and wide bandwidth emission spectra [11-15]. Recently, phosphate glasses have attained great attention in synthesis, structure and physical properties due to their high density and high dielectric constant [16-18].

The present work reports on the preparation and characterization of rare earth doped heavy metal oxide (HMO) glass systems for lasing materials. I have studied on the Thermal, absorption, Excitation and fluorescence properties of Ho<sup>3+</sup> doped zinc lithium alumino potassiumniobate borophosphate glasses. The intensities of the transitions for the rare earth ions have been estimated successfully using the Judd-Ofelt theory, The laser parameters such as radiative probabilities( $A$ ), branching ratio ( $\beta$ ), radiative life

time( $\tau_R$ ) and stimulated emission cross section( $\sigma_p$ ) are evaluated using J.O. intensity parameters ( $\Omega_\lambda$ ,  $\lambda=2,4$  and 6).

## Experimental:

### Preparation of glasses:

The following Ho<sup>3+</sup>doped borosilicate glass samples (35-x) P<sub>2</sub>O<sub>5</sub>:10ZnO:10Li<sub>2</sub>O:10 Al<sub>2</sub>O<sub>3</sub>:10K<sub>2</sub>O: 10Nb<sub>2</sub>O<sub>3</sub>: 15B<sub>2</sub>O<sub>3</sub>: x Ho<sub>2</sub>O<sub>3</sub>. (where x=1,1.5 and 2 mol%) have been prepared by melt-quenching method. Analytical reagent grade chemical used in the present study consist of P<sub>2</sub>O<sub>5</sub>, ZnO, Li<sub>2</sub>O, Al<sub>2</sub>O<sub>3</sub>, K<sub>2</sub>O, Nb<sub>2</sub>O<sub>3</sub>, B<sub>2</sub>O<sub>3</sub> and Ho<sub>2</sub>O<sub>3</sub>. They were thoroughly mixed by using an agate pestle mortar. then melted at 1005<sup>o</sup>C by an electrical muffle furnace for 2h., After complete melting, the melts were quickly poured in to a preheated stainless steel mould and annealed at temperature of 250<sup>o</sup>C for 2h to remove thermal strains and stresses. Every time fine powder of cerium oxide was used for polishing the samples. The glass samples so prepared were of good optical quality and were transparent. The chemical compositions of the glasses with the name of samples are summarized in **Table 1**.

**Table 1:** Chemical composition of the glasses

Sample	Glass composition (mol %)
ZLAPNBP (UD)	35P <sub>2</sub> O <sub>5</sub> :10ZnO:10Li <sub>2</sub> O:10Al <sub>2</sub> O <sub>3</sub> :10K <sub>2</sub> O:10Nb <sub>2</sub> O <sub>3</sub> :15B <sub>2</sub> O <sub>3</sub>
ZLAPNBP (HO1)	34P <sub>2</sub> O <sub>5</sub> : 10ZnO: 10Li <sub>2</sub> O: 10Al <sub>2</sub> O <sub>3</sub> : 10K <sub>2</sub> O: 10Nb <sub>2</sub> O <sub>3</sub> : 15B <sub>2</sub> O <sub>3</sub> :1 Ho <sub>2</sub> O <sub>3</sub>
ZLAPNBP (HO1.5)	33.5P <sub>2</sub> O <sub>5</sub> : 10ZnO: 10Li <sub>2</sub> O: 10Al <sub>2</sub> O <sub>3</sub> : 10K <sub>2</sub> O:10Nb <sub>2</sub> O <sub>3</sub> :15B <sub>2</sub> O <sub>3</sub> :1.5Ho <sub>2</sub> O <sub>3</sub>
ZLAPNBP (HO2)	33P <sub>2</sub> O <sub>5</sub> : 10ZnO: 10Li <sub>2</sub> O: 10Al <sub>2</sub> O <sub>3</sub> : 10K <sub>2</sub> O:10Nb <sub>2</sub> O <sub>3</sub> :15B <sub>2</sub> O <sub>3</sub> : 2 Ho <sub>2</sub> O <sub>3</sub>

ZLAPNBP (UD) -Represents undoped Zinc Lithium Alumino Potassiumniobate Borophosphate glass specimen.

ZLAPNBP (HO)-Represents Ho<sup>3+</sup> doped Zinc Lithium Alumino Potassiumniobate Borophosphate glass specimens.

### Theory:

#### Oscillator Strength:

The intensity of spectral lines are expressed in terms of oscillator strengths using the relation [21].

$$f_{\text{expt.}} = 4.318 \times 10^{-9} \int \epsilon(\nu) d\nu \quad (1)$$

where,  $\epsilon(\nu)$  is molar absorption coefficient at a given energy  $\nu$  (cm<sup>-1</sup>), to be evaluated from Beer–Lambert law.

Under Gaussian Approximation, using Beer–Lambert law, the observed oscillator strengths of the absorption bands have been experimentally calculated [22], using the modified relation:

$$P_m = 4.6 \times 10^{-9} \times \frac{1}{cl} \log \frac{I_0}{I} \times \Delta\nu_{1/2} \quad (2)$$

where,  $c$  is the molar concentration of the absorbing ion per unit volume,  $l$  is the optical path length,  $\log I_0/I$  is optical density and  $\Delta\nu_{1/2}$  is half band width.

### Judd-Ofelt Intensity Parameters

According to Judd [23] and Ofelt [24] theory, independently derived expression for the oscillator strength of the induced forced electric dipole transitions between an initial J manifold  $|4f^N(S, L) J\rangle$  level and the terminal J' manifold  $|4f^N(S', L') J'\rangle$  is given by:

$$\frac{8\pi^2 mc \bar{\nu}}{3h(2J+1)n} \left[ \frac{(n^2+2)^2}{9} \right] \times S(J, J') \quad (3)$$

Where, the line strength  $S(S', L')$  is given by the equation

$$S(J, J') = e^2 \sum \Omega_\lambda \langle 4f^N(S, L) J \| U^{(\lambda)} \| 4f^N(S', L') J' \rangle^2 \quad (4)$$

$\lambda = 2, 4, 6$

In the above equation  $m$  is the mass of an electron,  $c$  is the velocity of light,  $\bar{\nu}$  is the wave number of the transition,  $h$  is Planck's constant,  $n$  is the refractive index,  $J$  and  $J'$  are the total angular momentum of the initial and final level respectively,  $\Omega_\lambda$  ( $\lambda = 2, 4, 6$ ) are known as Judd-Ofelt intensity parameters.

### Radiative Properties

The  $\Omega_\lambda$  parameters obtained using the absorption spectral results have been used to predict radiative properties such as spontaneous emission probability ( $A$ ) and radiative life time ( $\tau_{rad}$ ), and laser parameters like fluorescence branching ratio ( $\beta_R$ ) and stimulated emission cross section ( $\sigma_p$ ).

The spontaneous emission probability from initial manifold  $|4f^N(S', L') J'\rangle$  to a final manifold  $|4f^N(S, L) J\rangle$  is given by:

$$A[(S', L') J'; (S, L) J] = \frac{64 \pi^2 \bar{\nu}^3}{3h(2J'+1)} \left[ \frac{n(n^2+2)^2}{9} \right] \times S(J', J) \quad (5)$$

where,  $S(J', J) = e^2 [\Omega_2 \| U^{(2)} \|^2 + \Omega_4 \| U^{(4)} \|^2 + \Omega_6 \| U^{(6)} \|^2]$

The fluorescence branching ratio for the transitions originating from a specific initial manifold  $|4f^N(S', L') J'\rangle$  to a final many fold  $|4f^N(S, L) J\rangle$  is given by

$$\beta[(S', L') J'; (S, L) J] = \sum \frac{A[(S', L') J'; (\bar{S}, \bar{L}) \bar{J}]}{A[(S', L') J'; (\bar{S}, \bar{L}) \bar{J}]} \quad (6)$$

$S, L, J$  where, the sum is over all terminal manifolds.

The radiative life time is given by

$$\tau_{rad} = \sum A[(S', L') J'; (S, L) J] = A_{Total}^{-1} \quad (7)$$

$S, L, J$  where, the sum is over all possible terminal manifolds. The stimulated emission cross-section for a transition from an initial manifold  $|4f^N(S', L') J'\rangle$  to a final manifold  $|4f^N(S, L) J\rangle$  is expressed as

$$\sigma_p(\lambda_p) = \left[ \frac{\lambda_p^4}{8\pi c n^2 \Delta\lambda_{eff}} \right] \times A[(S', L') J'; (\bar{S}, \bar{L}) \bar{J}] \quad (8)$$

where,  $\lambda_p$  the peak fluorescence wavelength of the emission band and  $\Delta\lambda_{eff}$  is the effective fluorescence line width.

### Nephelauxetic Ratio ( $\beta'$ ) and Bonding Parameter ( $b^{1/2}$ )

The nature of the R-O bond is known by the Nephelauxetic Ratio ( $\beta'$ ) and Bonding

Parameters ( $b^{1/2}$ ), which are computed by using following formulae [25, 26]. The Nephelauxetic Ratio is given by

$$\beta' = \frac{\nu_g}{\nu_a} \quad (9)$$

where,  $\nu_a$  and  $\nu_g$  refer to the energies of the corresponding transition in the glass and free ion, respectively. The values of bonding parameter  $b^{1/2}$  are given by

$$b^{1/2} = \left[ \frac{1-\beta'}{2} \right]^{1/2} \quad (10)$$

## Results and Discussion:

### XRD Measurement

Figure 1 presents the XRD pattern of the sample contain –  $P_2O_5$  which is show no sharp Bragg's peak, but only a broad diffuse hump around low angle region. This is the clear indication of amorphous nature within the resolution limit of XRD instrument.

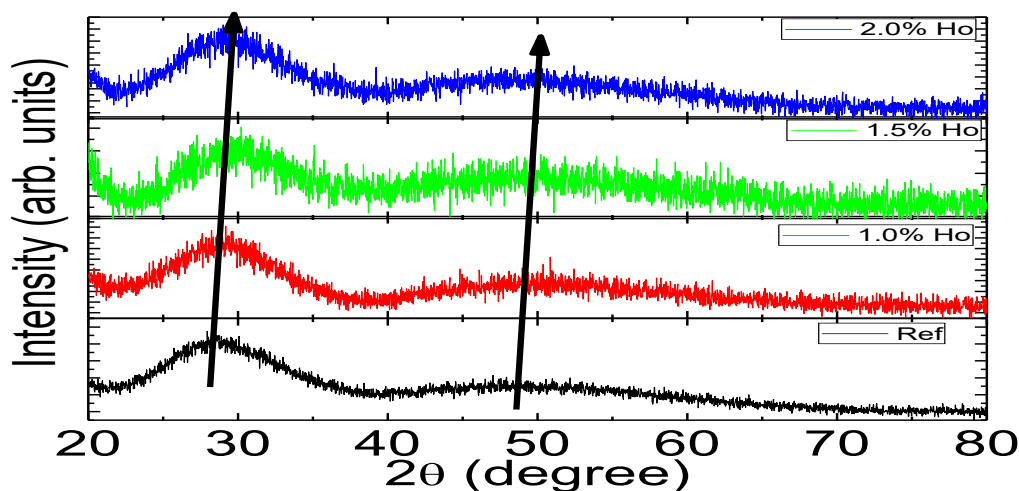


Fig. 1: X-ray diffraction pattern of  $P_2O_5$ : ZnO: Li<sub>2</sub>O: Al<sub>2</sub>O<sub>3</sub>: K<sub>2</sub>O: Nb<sub>2</sub>O<sub>3</sub>:B<sub>2</sub>O<sub>3</sub>: Ho<sub>2</sub>O<sub>3</sub>

### Thermal Properties

Fig. 2 depicts the DTA thermogram of powdered ZLAPNBP sample show an endothermic peak corresponding to glass transition event followed by an exothermic peak related to crystallization event. The glass transition temperature ( $T_g$ ), onset crystallization temperature ( $T_x$ ), crystallization temperature ( $T_c$ ) were estimated to be 516<sup>0</sup>C, 582<sup>0</sup>C and 595<sup>0</sup>C respectively. From the measured value of  $T_g$ ,  $T_x$  and  $T_c$ , the glass stability factor ( $\Delta T = T_x - T_g$ ) has been determined to be 66<sup>0</sup>C indicating the good stability of the glass.

Obtained results indicate that by increasing the amount of mol%  $\text{Ho}_2\text{O}_3$ , the  $T_g$  of the samples also increases, the small increase of  $T_g$  in these glasses shows that the structure is strongly and progressively modified. The thermal stabilities  $\Delta T$  of the ZLAPNBP reference glass and  $\text{Ho}^{3+}$ doped ZLAPNBP glass has been evaluated from their  $T_g$ ,  $T_c$  and  $T_x$  values, the results are listed out in Table 2. Hruby's parameter also calculated by using eq. (11), the greater values of the Hruby's parameter indicate higher glass forming tendency, the values of  $H$  in our glasses increased with the addition of the  $\text{Ho}_2\text{O}_3$ . Eqs. (12) and (13) present the GS parameter of Weinberg [25] and Lu and Liu [26], respectively.

$$H = \frac{T_x - T_g}{T_c - T_x} \quad (11)$$

$$K_W = \frac{T_x - T_g}{T_c} \quad (12)$$

$$K_{LL} = \frac{T_x}{T_g + T_c} \quad (13)$$

**Table 2:** Thermal parameters determined from the DTA traces of ZLAPNBP (HO) glasses.

Sample Name	% $\text{Sm}_2\text{O}_3$	$T_g$ °C	$T_x$ °C	$T_c$ °C	$\Delta T$	H	$K_W$	$K_{LL}$
ZLAPNBP (HO 1.0)	1	516	582	595	66	5.076	0.1109	0.5231
ZLAPNBP (HO 1.5)	1.5	518	585	598	67	5.153	0.1120	0.5242
ZLAPNBP (HO 02)	2	522	592	605	70	5.231	0.1157	0.5253

### Absorption Spectrum

The absorption spectra of  $\text{Ho}^{3+}$ doped ZLAPNBP glass specimens have been presented in Figure 3 in terms of optical density versus wavelength. Twelve absorption bands have been observed from the ground state  $^5I_8$  to excited states  $^5I_5$ ,  $^5I_4$ ,  $^5F_5$ ,  $^5F_4$ ,  $^5F_3$ ,  $^3K_8$ ,  $^5G_6$ ,  $(^5G, ^3G)_5$ ,  $^5G_4$ ,  $^5G_2$ ,  $^5G_3$ , and  $^3F_4$  for  $\text{Ho}^{3+}$ doped ZLAPNBP glasses.

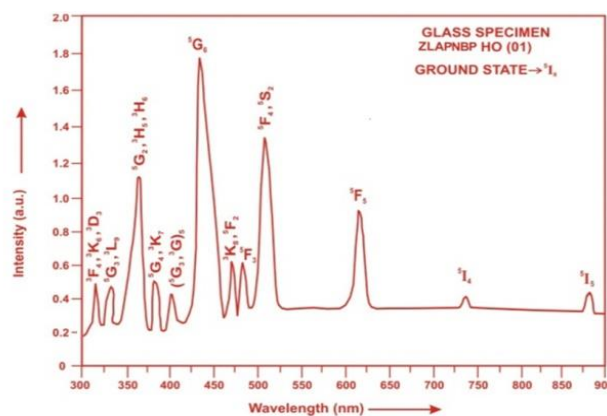
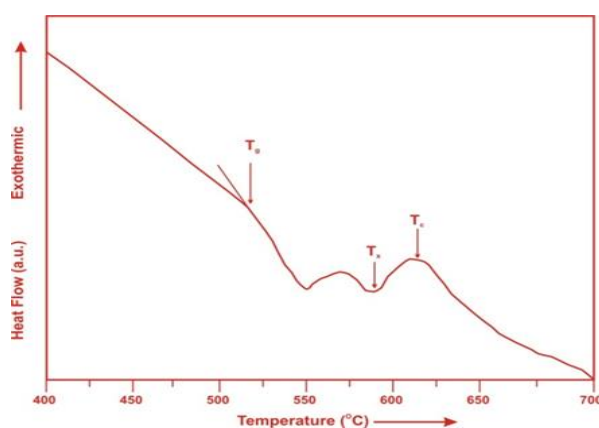


**Fig. 2.** DTA thermogram of powdered ZLAPNBP sample. **Fig. 3:** Absorption spectrum of  $\text{Ho}^{3+}$ doped ZLAPNBP HO (01) glass.

The experimental and calculated oscillator strength for  $\text{Ho}^{3+}$  ions in ZLAPNBP glasses are given in Table 3.

**Table 3:** Measured and calculated oscillator strength ( $P_m \times 10^{+6}$ ) of  $\text{Ho}^{3+}$  ions in ZLAPNBP glasses.

Energy level from $^5\text{I}_8$	Glass ZLAPNBP (HO01)		Glass ZLAPNBP (HO1.5)		Glass ZLAPNBP (HO02)	
	$P_{\text{exp}}$	$P_{\text{cal}}$	$P_{\text{exp}}$	$P_{\text{cal}}$	$P_{\text{exp}}$	$P_{\text{cal}}$
$^5\text{I}_5$	0.53	0.24	0.48	0.24	0.45	0.24
$^5\text{I}_4$	0.06	0.02	0.05	0.02	0.04	0.02
$^5\text{F}_5$	3.66	2.78	3.62	2.75	3.58	2.72
$^5\text{F}_4$	4.60	4.29	4.56	4.25	4.52	4.22
$^5\text{F}_3$	1.53	2.37	1.49	2.36	1.45	2.34
$^3\text{K}_8$	1.45	1.97	1.42	1.94	1.38	1.92
$^5\text{G}_6$	26.68	26.63	25.28	25.26	24.78	24.78
$(^5\text{G}, ^3\text{G})_5$	3.82	1.72	3.76	1.68	3.72	1.67
$^5\text{G}_4$	0.08	0.61	0.06	0.60	0.05	0.59
$^5\text{G}_2$	5.62	5.61	5.58	5.36	5.54	5.27
$^5\text{G}_3$	1.50	1.40	1.46	1.37	1.42	1.35
$^3\text{F}_4$	1.38	4.20	1.32	4.12	1.27	4.08
r.m.s. deviation	$\pm 1.1031$	--	$\pm 1.0975$	--	$\pm 1.0977$	--

Computed values of  $F_2$ , Lande' parameter ( $\xi_{4f}$ ), Nephlauxetic ratio ( $\beta'$ ) and bonding parameter ( $b^{1/2}$ ) for  $\text{Ho}^{3+}$  ions in ZLAPNBP glass specimen are given in Table 4.

**Table 4:**  $F_2$ ,  $\xi_{4f}$ ,  $\beta'$  and  $b^{1/2}$  parameters for Holmium doped glass specimen.

Glass Specimen	$F_2$	$\xi_{4f}$	$\beta'$	$b^{1/2}$
$\text{Ho}^{3+}$	358.82	1258.16	0.9337	0.1821

In the Zinc Lithium Alumino Potassiumniobate Borophosphate glasses (ZLAPNBP)  $\Omega_2$ ,  $\Omega_4$  and  $\Omega_6$  parameters decrease with the increase of x from 1 to 2 mol%. The order of magnitude of Judd-Ofelt intensity parameters is  $\Omega_2 > \Omega_6 > \Omega_4$  for all the glass specimens. The spectroscopic quality factor ( $\Omega_4 / \Omega_6$ )

related with the rigidity of the glass system has been found to lie between 0.6181 and 0.6294 in the present glasses. The values of Judd-Ofelt intensity parameters are given in **Table 5**.

**Table 5:** Judd-Ofelt intensity parameters for Ho<sup>3+</sup> doped ZLAPNBP glass specimens.

Glass Specimen	$\Omega_2(\text{pm}^2)$	$\Omega_4(\text{pm}^2)$	$\Omega_6(\text{pm}^2)$	$\Omega_4/\Omega_6$	Ref.
ZLAPNBP (HO01)	6.576	1.369	2.175	0.6294	[P.W.]
ZLAPNBP (HO1.5)	6.186	1.338	2.160	0.6194	[P.W.]
ZLAPNBP (HO02)	6.051	1.324	2.142	0.6181	[P.W.]

### Excitation Spectrum

The Excitation spectra of Ho<sup>3+</sup>-doped ZLAPNBP glass specimens have been presented in Figure 4 in terms of Excitation Intensity versus wavelength. The excitation spectrum was recorded in the spectral region 325–525 nm fluorescence at 545nm having different excitation band centered at 350,419, 452, 472and 485 nm are attributed to the <sup>5</sup>G<sub>3</sub>, (<sup>5</sup>G, <sup>3</sup>G)<sub>5</sub>, <sup>5</sup>G<sub>6</sub>, <sup>3</sup>K<sub>8</sub> and <sup>5</sup>F<sub>3</sub> transitions, respectively. The highest absorption level is <sup>5</sup>G<sub>6</sub> and is at 452nm. So this is to be chosen for excitation wavelength.

### Fluorescence Spectrum

The fluorescence spectrum of Ho<sup>3+</sup>-doped in zinc lithium alumino potassiumniobate borophosphate glass is shown in Figure 5. There are five broad bands observed in the Fluorescence spectrum of Ho<sup>3+</sup>-doped zinc lithium alumino potassiumniobate glass. The wavelengths of these bands along with their assignments are given in Table 6. The peak with maximum emission intensity appears at 555 nm and corresponds to the (<sup>5</sup>F<sub>4</sub>→<sup>5</sup>I<sub>8</sub>) transition.

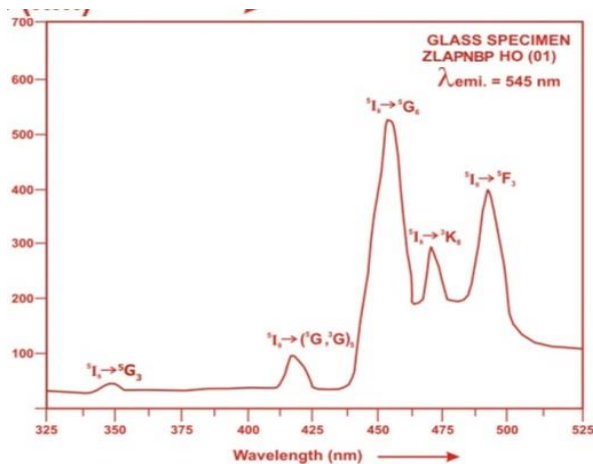


**Fig. 4:** Excitation spectrum of doped with Ho<sup>3+</sup> ZLAPNBP glasses.

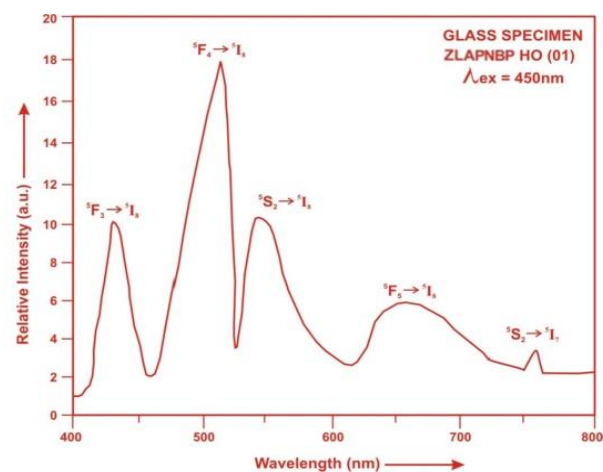


**Fig. 5:** Fluorescence spectrum of doped with Ho<sup>3+</sup> ZLAPNBP glasses

## Conclusion:

In the present study, the glass samples of composition  $(35-x) \text{P}_2\text{O}_5: 10\text{ZnO}:10\text{Li}_2\text{O}:10 \text{Al}_2\text{O}_3: 10\text{K}_2\text{O}: 10\text{Nb}_2\text{O}_3: 15\text{B}_2\text{O}_3:x\text{Ho}_2\text{O}_3$ . (where  $x = 1, 1.5$  and  $2 \text{mol } \%$ ) have been prepared by melt-quenching method. The value of stimulated emission cross-section ( $\sigma_p$ ) is found to be maximum for the transition ( $^5\text{F}_4 \rightarrow ^5\text{I}_8$ ) for glass ZLAPNBP (HO 01), suggesting that glass ZLAPNBP (HO 01) is better compared to the other two glass systems ZLAPNBP (HO1.5) and ZLAPNBP (HO02). The greater values of the Hruby's parameter indicate higher glass forming tendency.

## Conflict of Interest:

The authors declared that they have no conflict of interest.

## References:

- [1] Monisha, M, Nancy, Ashwitha, Souza, D., legde, Vinod, Prabhu, N. S. and Sayyed, M.I. (2020). Dy<sup>3+</sup> doped SiO<sub>2</sub>- B<sub>2</sub>O<sub>3</sub>-Al<sub>2</sub>O<sub>3</sub>-NaF-ZnF<sub>2</sub> glasses : An exploration of optical and gamma radiation shielding features, Current Applied Physics 20(11), 1207-1210.
- [2] Prabhu, N. S., Hegde, V., Sayyed, M.I., Agar, O. and Kamath, S. D. (2019). Investigations on structural and radiation shielding properties of Er<sup>3+</sup> doped zinc bismuth borate glasses, Materials chemistry and physics, 230, 267-276.
- [3] Patwari, R., Eraiah, B. (2019). Optical and Plasmonic properties of Er<sup>3+</sup> and silver co-doped borate nano- composite glasses, Materials Research Express 6(11), 116218.
- [4] Sienkiewicz, P., Palkowslea, A., pietr-zyeki, M., Romanczunk, P., Zmojda, J., koxhanowicz, M. and Dorosz, D. (2014). Multicolor up conversion emission in tellurite glasses co-doped with rare earth ions for white LED applications, Photonics Applications in Astronomy, Communications, Industry and High Energy physics experiments.
- [5] Liggins, K., Edwards, V. M. and Reddy, B. R. (2017). White light Emission characteristics of rare earth ion doped sodium borate glass," Optical Components and materials.
- [6] El Maaref, A.A., Badr, S., Shaaban, Kh.S., Abdel Wahab, E.A. and Elokr, M.M. (2019). Optical properties and radiative rates of Nd<sup>3+</sup> doped zinc- sodium phosphate Glasses," Journal of rare Earth, 37, 253-259.
- [7] Ratnakaram, V. C., Reddy Prasad, V., Babu, S. and Kumar, V. V. R. K. (2016). "Luminescence performance of Eu<sup>3+</sup> doped lead free zinc phosphate glasses for red emission," Bulletin of Materials Science 39, 1065-1072.
- [8] Babu, S. S., Babu, P., Jayasankar, C.K., Sievers, W. and Wortmann, G. (2007). Optical absorption and photoluminescence studies of Eu<sup>3+</sup> doped phosphate and fluorphosphate glasses, Journal of luminescence, 126, 109-120.
- [9] Venkatramu, V., Vijaya, R., Luis, S.F., Babu, P., Jayasankar, C.K., Lavin, V. and Dhareshwar, L.J. (2011). Optical properties of Yb<sup>3+</sup> doped phosphate laser glasses," Journal of Alloys and Compounds, 509, 5084-5089.
- [10] Christopher, A.G., Kalnnis, H., Ebendorff, H., Nigel A Spooner and Tanya M, Marno, (2011). Optically stimulated luminescence in fluoride phosphate glass for radiation dosimetry, Journal of the American Ceramic Society , 94(2), 474-477.
- [11] Wojciench, A., Pisarski Lidia, Zur, Tomasz, Goryczka, Marta, S. and Piesarska, Joanna (2014). Structure and Spectroscopy of rare earth doped lead phosphate glasses. (Eu, Tb, Dy, Er), Journal of Alloys and Compound 587, 90-98(2014).



- [12] Seshadri, M., Radha, M., Barbosa, C., Cordeiro, C.M.B. and Ratnaka, Y.C. (2015). Effect of ZnO on spectroscopic properties of Sm<sup>3+</sup> doped zinc phosphate glasses, *Physica B: Condensed matter* 459, 79-87.
- [13] Marzouk, M.A., ElBatel, H. A., Hamdy, Y.M. and Ezz-Eldin, F. M. (2019). Collective Optical, FTIR and Photoluminescence Spectra of CeO<sub>2</sub> and Sm<sub>2</sub>O<sub>3</sub> Doped Na<sub>2</sub>O-ZnO-P<sub>2</sub>O<sub>5</sub> Glasses, *International Journal of Optics*.
- [14] Mitra, S. and Jana, S. (2015). Intense orange emission in Pr<sup>3+</sup> doped lead phosphate glass, *Journal of physics and chemistry of solids* 85, 245-253.
- [15] Amlah S., Azmi, M., Sahar, M.R., Ghoshal, S.K. and Arifin, R. (2015). Modification of structural and physical properties of samarium doped zinc phosphate glasses due to the inclusion of nickel oxide nanoparticles, *Journal of Non crystalline Solids* 411, 53-58.
- [16] Chen, Y., Chen, G.H., Liu, X.Y. and Yang, T. (2018). Enhanced up – conversion luminescence and optical thermometry characteristics of Er<sup>3+</sup>/ Yb<sup>3+</sup> co-doped transparent phosphate Glass Ceramics, *Journal of luminescence* 195, 314-320.
- [17] Liyu Hao, Manting Pei, Tie Yang, Chengguo Ming (2020). Double sensitivity temperature sensor based on excitation intensity ratio of Eu<sup>3+</sup> doped phosphate glass ceramic, *Optik* 204, 164188.
- [18] Dutebo, M. T., Shashikala, H.D. (2020). Influence of (Er<sup>3+</sup>, La<sup>3+</sup>, Ce<sup>4+</sup>) additions on physical and optical properties of 50 CaO- 50 P<sub>2</sub>O<sub>5</sub> glasses, *Physics B: Condensed Matter* 597, 412358.
- [19] Gorller-Walrand, C. and Binnemans, K. (1988) Spectral Intensities of f-f Transition. In: Gshneidner Jr., K.A. and Eyring, L., Eds., *Handbook on the Physics and Chemistry of Rare Earths*, Vol. 25, Chap. 167, North-Holland, Amsterdam, 101.
- [20] Sharma, Y.K., Surana, S.S.L. and Singh, R.K. (2009). Spectroscopic Investigations and Luminescence Spectra of Sm<sup>3+</sup> Doped Soda Lime Silicate Glasses. *Journal of Rare Earths*, 27, 773.
- [21] Judd, B.R. (1962). Optical Absorption Intensities of Rare Earth Ions. *Physical Review*, 127, 750.
- [22] Ofelt, G.S. (1962). Intensities of Crystal Spectra of Rare Earth Ions. *The Journal of Chemical Physics*, 37, 511.
- [23] Sinha, S.P. (1983). Systematics and properties of lanthanides, Reidel, Dordrecht.
- [24] Krupke, W.F. (1974). Induced- emission cross-section in neodymium laser glasses. *IEEE J. Quantum electron* QE-10, 450-457.
- [25] Weinberg, M.C. (1994). Experimental test of surface nucleated crystal growth model in lithium diborate glass, *Phys. Chem. Glasses* 35, 119.
- [26] Lu, Z.P. and Liu, C.T. (2003). Glass Formation Criterion for Various Glass-Forming Systems *Phys. Rev. Lett.* 91, 11550.

**Table 6:** Emission peak wave lengths ( $\lambda_p$ ), radiative transition probability ( $A_{rad}$ ), branching ratio ( $\beta$ ), stimulated emission cross-section ( $\sigma_p$ ) and radiative life time ( $\tau_R$ ) for various transitions in  $\text{Ho}^{3+}$  doped ZLAPNBP glasses.

Transition	ZLAPNBP (HO 01)					ZLAPNBP (HO 1.5)				ZLAPNBP (HO 02)			
	$\lambda_{max}$ (nm)	$A_{rad}(s^{-1})$	$\beta$	$\sigma_p (10^{-20} \text{ cm}^2)$	$\tau_R(\mu s)$	$\lambda_{max}$ (nm)	$A_{rad}$ ( $s^{-1}$ )	$\beta$	$\sigma_p (10^{-20} \text{ cm}^2)$	$A_{rad}(s^{-1})$	$\lambda_{max}$ (nm)	$A_{rad}$ ( $s^{-1}$ )	$\beta$
$^5F_3 \rightarrow ^5I_8$	435	4086.30	0.2641	0.5233	6464.10	4069.01	0.2648	0.509	6506.51	4040.35	0.2646	0.490	6549.07
$^5F_4 \rightarrow ^5I_8$	501	6517.41	0.4213	1.146		6467.20	0.4208	1.124		6428.04	0.4210	1.083	
$^5S_2 \rightarrow ^5I_8$	555	1706.85	0.1103	0.396		1698.46	0.1105	0.389		1686.75	0.1105	0.381	
$^5F_5 \rightarrow ^5I_8$	652	1864.64	0.1205	0.710		1846.06	0.1201	0.693		1833.92	0.1201	0.675	
$^5S_2 \rightarrow ^5I_7$	761	1294.87	0.08370	0.948		1288.50	0.08384	0.934		1280.31	0.08385	0.910	